1 # Transport pathways of carbon monoxide from Indonesian fire
2 # pollution to a subtropical high-altitude mountain site in western
3 # North Pacific

4 Saginela Ravindra Babu[1*], Chang-Feng Ou-Yang[1], Stephen M. Griffith[1], Shantanu Kumar Pani[1],

5 Steven Soon-Kai Kong[1], and Neng-Huei Lin[1,2*]

6

7 [1]Department of Atmospheric Sciences, National Central University, Taoyuan 32001, Taiwan.

8 [2]Center for Environmental Monitoring and Technology, National Central University, Taoyuan

9 32001, Taiwan.

10 Correspondence to: S. Ravindra Babu (baburavindra595@gmail.com) and Neng-Huei Lin
11 (nhlin@cc.ncu.edu.tw).

12 **Abstract:** Dry conditions associated with El Niño and a positive Indian Ocean Dipole (IOD) are

13 known to have caused major fire pollution events and intense carbon emissions over a vast spatial

14 expanse of Indonesia in October 2006 and 2015. During these two events, a substantial increase in

15 carbon monoxide (CO) mixing ratio was detected by in-situ measurements at Lulin Atmospheric

16 Background Station (LABS, 23.47°N 120.87°E, 2,862 m ASL) in Taiwan, the only background

17 station in the subtropical western North Pacific region. Compared to the long-term October mean

18 (2006-2021), CO was elevated by ~47.2 ppb (37.2%) and ~36.7 ppb (28.9%) in October 2006 and

19 2015, respectively. This study delineates plausible pathways for CO transport from Indonesia to

20 LABS using MOPITT CO observations and MERRA-2 reanalysis products (winds and

21 geopotential height (GpH)). Two simultaneously occurring transport pathways were identified: (i)

22 horizontal transport in the free troposphere and (ii) vertical transport through the Hadley

23 circulation (HC). The GpH analysis of both events revealed the presence of a high-pressure

24 anticyclone over the northern part of the South China Sea (SCS), which played an important role

25 in the free tropospheric horizontal transport of CO. In this scenario, CO in the free troposphere is

26 transported on the western edge of the high-pressure system and then driven by subtropical

27 westerlies to LABS. Simultaneously, uplifted CO over Indonesia can enter the HC and transfer to

28 subtropical locations such as LABS. The vertical cross-section of MOPITT CO and MERRA-2

29 vertical pressure velocity supported the transport of CO through the HC. Further, the results

30 revealed a distinct HC strength in two events (higher in 2006 compared to 2015) due to the

Atmospheric
Chemistry
and Physics
Discussions

31   different El Niño conditions. Overall, the present findings can provide some insights into

32   understanding the regional transport of pollution over Southeast Asia and the role of climate

33   conditions on transport pathways.

34   **Keywords:** Indonesian fire pollution; Carbon monoxide; Lulin Atmospheric Background Station;

35   Hadley circulation

36   **1. Introduction**

37   Fire activity over Southeast Asia (SEA), particularly over the Maritime Continent (MC,

38   including Indonesia), is a severe environmental problem that causes widespread regional pollution

39   in the lower troposphere and impacts atmospheric chemistry, air quality, and climate at regional

40   to global scales. Over the MC, fires occur predominantly in the dry season (August to October)

41   and particularly during the periods of drought, often associated with the positive phase of El Niño-

42   Southern Oscillation (ENSO) events (Duncan et al., 2003a; van der Werf et al.,2008, 2017; Field

43   et al., 2009, 2016). A recent study has also highlighted the role of the Indian Ocean Dipole on MC

44   fire activity (Pan et al., 2018). For example, dry conditions associated with the extreme 2015/16

45   El Niño and weak 2006/07 El Niño events led to increased fire activity over Indonesia and the

46   wider MC (van der Werf et al.,2008; Chandra et al., 2009; Nassar et al., 2009; Huijnen et al.,

47   2016; Field et al., 2016). Due to these intense fires, an enormous amount of carbon emissions

48   was released into the atmosphere in the form of carbon dioxide (CO_2), carbon monoxide (CO),

49   and methane (CH_4) (Huijnen et al., 2016; Field et al., 2016; Parker et al., 2016; Heymann et al.,

50   2017). These two Indonesian fire events and the associated impacts on carbon emissions, trace gas

51   and aerosol composition, and air quality has been extensively discussed in the literature (Chandra

52   et al., 2006; Logan et al., 2008; Chandra et al., 2009; Nassar et al., 2009; Huijnen et al., 2016;

53   Field et al., 2016; Heymann et al., 2017; Ravindra Babu et al., 2019). For example, the fire carbon

54   emissions during September-October 2015 over Maritime SEA were the largest since 1997

55   (Huijnen et al., 2016). By using Greenhouse gases Observing SATellite (GOSAT) data, Parker et

56   al. (2016) reported the strong enhancement of CO_2 and CH_4 over the Indonesian region.

57   CO is a significant emission from the combustion of fossil fuels and biomass (forest and

58   savanna fires, biofuel use, and waste burning) and is widely used as a tropospheric tracer for these

59   sources (Ou-Yang et al., 2014; Pani et al., 2019). Inter-annual variability of CO in the tropics and

60   sub-tropics is largely linked to year-by-year changes in biomass burning (BB) emissions.

61   Indonesian fires often emit large quantities of CO by incomplete combustion associated with the

62   occurrence of peat fire pollution. Although CO is not a direct greenhouse gas (GHG), it does have

63   a global warming potential due to its chemical reactions in the atmosphere. For instance, CO

64   oxidation produces CO_2 and indirectly ozone (O_3), both of which are GHGs, and depletes hydroxyl

65   radical (OH) concentrations, thus extending the lifetime of CH_4, another GHG in the atmosphere

66   (IPCC, 2013). The lifetime of CO in the free troposphere is ∼ two months, thus can be a tracer

67   from polluted upwind regions to remote downwind areas (Cooper et al., 2012). Some of the studies

68   reported the influence of Indonesian fire activity and the transport of CO from Indonesia to the

69   Indian Ocean, Southern Pacific, and western Pacific Ocean (Matsueda and Inoue, 1999; Pochanart

70   and Akimoto, 2003; Nara et al., 2011; Matsueda et al., 2002, 2019). However, the underlying

71   transport mechanisms sending this fire pollution to downwind northern hemisphere subtropical

72   locations, particularly transport to high-altitude background locations in the western north Pacific

73   are still unclear.

74   As shown in **Figure 1**, the Lulin Atmospheric Background Station (LABS, 23.47°N

75   120.87°E, 2862 m ASL) located in central Taiwan was constructed in 2006 and is the only high-

76   altitude background station in the western Pacific region for monitoring the long-term variability

77   of atmospheric compositions and also studying the influence of continental outflow and long-range

78   transported pollution (Lin et al., 2013; Ou-Yang et al., 2014, 2022; Ravindra Babu et al., 2022).

79   The LABS is often found within the free troposphere, making it an ideal site for measuring long-

80   range transport of air pollutants, complementing the global network of the Global Atmospheric

81   Watch (GAW) in the East Asia region where no other high-altitude background station is available

82   (Ou-Yang et al., 2014, 2022). In the framework of Seven South-East Asian Studies (7-SEAS, Reid,

83   et al., 2013; Lin et al., 2013; Wang et al., 2015), several studies at LABS have reported on the

84   long-range transport of northern peninsular Southeast Asia (PSEA) BB pollutants to Taiwan

85   through the low-level jet (LLJ) and the related impacts on air quality and chemistry over Taiwan

86   (Ou-Yang et al., 2012, 2014; Lin et al., 2013; Chuang et al., 2016; Chi et al., 2016; Tsay et al.,

87   2016; Hsiao et al., 2016; Lin et al., 2017; Park et al., 2019; Pani et al., 2016, 2019; Huang et al.,

88   2019; Huang et al., 2020; Ravindra Babu et al., 2022). However, to date, no studies have shown

89   the potential influence of Indonesian fire activities on LABS measurements and the BB pollution

90   from Indonesian fires reaching LABS. Surprisingly, the extensive fire events in 2006 and 2015

91 allowed us to track CO concentrations from the Indonesian peat fires to LABS in Taiwan. By

92 combining in-situ and satellite CO measurements and large-scale circulation parameters from

93 reanalysis products, we identified plausible transport pathways from Indonesia to LABS.
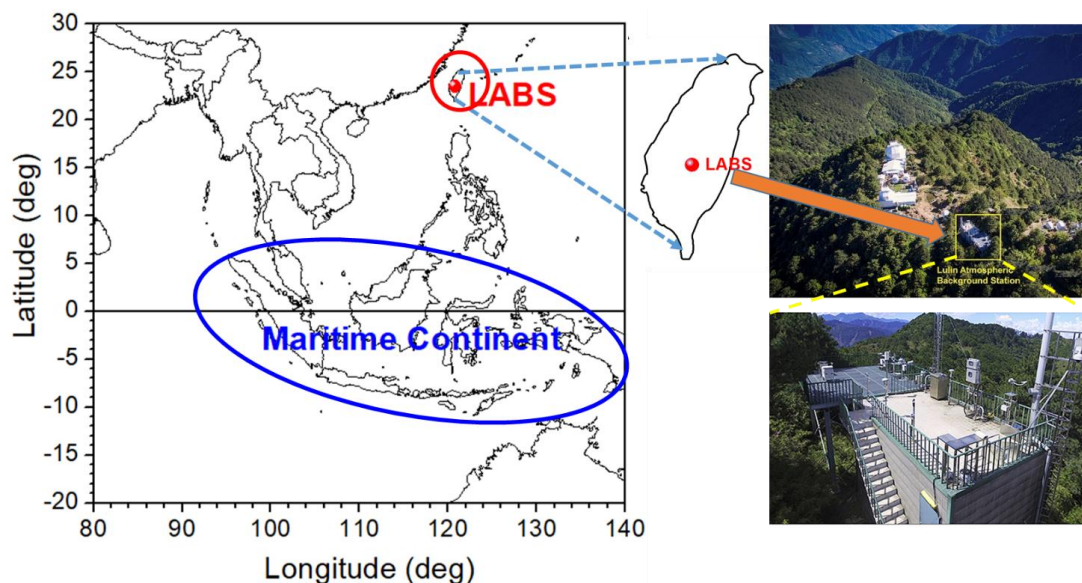
95 **Figure 1**. Geographic location of the Maritime Continent and Lulin Atmospheric Background

96 Station (LABS, 23.47°N 120.87°E, 2862 m ASL), Taiwan.

97 **2. Data and methodology**

98 **2.1 In-situ measurements**

99   CO mixing ratios were measured by a nondispersive infrared (NDIR) analyzer (APMA-

100 360, Horiba, Japan) at LABS. Hourly averages of the 6-s data were analyzed in this study. The

101 detection limit of the NDIR is ~20 ppb (1σ) (Zellweger et al., 2009); more details about CO

102 measured at LABS can be found in Ou-Yang et. (2014). The magnitude of the CO concentration

103 enhancement in 2006 and 2015 above the long-term background was determined by comparing a

104 16-year average (2006-2021) of October CO data at LABS. We obtained the percentage change in

105 CO relative to the respective background using Equation 1:

106 $$\text{Relative change in percentage} = \left(\frac{x_{i} - \bar{x}}{\bar{x}}\right) \times 100 \qquad \text{(Eq. 1)}$$

107 where x_i represents the monthly mean of October in 2006 and 2015, and $\bar{x}$ is the corresponding

108 monthly long-term mean calculated using the data from 2006 to 2021 (Ou-Yang et al., 2014).

2.2 Satellite measurements

110 CO observations from the Measurement of Pollution in the Troposphere (MOPITT, version

111 8) instrument were also utilized in this study (Worden et al., 2010; Deeter et al., 2019). MOPITT

112 is a multi-channel Thermal InfraRed (TIR) and Near InfraRed (NIR) instrument operating onboard

113 sun-synchronous polar-orbiting NASA Terra satellite. V8 CO products, consisting of a CO profile

114 at ten pressure levels, have been validated; more details about the retrieval algorithm, validation,

115 and the uncertainties of MOPITT CO can be found in Deeter et al. (2019). In addition to the

116 MOPITT measurements, we utilized CO from the Atmospheric Infrared Sounder (AIRS) on the

117 NASA Aqua satellite, which provides CO at different vertical levels twice daily and near-global

118 coverage. AIRS uses wavenumbers 2,183-2,200 cm^{-1} (4.58-4.5 μm) for retrieving CO (McMillan

119 et al., 2005). Version 8, level 3 CO product, available at 1° ×1° resolution at various pressure

120 levels, was utilized in the present study. AIRS data were downloaded from the following website

121 https://disc.gsfc.nasa.gov/datasets/AIRS3STM_7.0 (AIRS project., 2019). AIRS sensitivity to CO

122 is broad and optimal in the mid-troposphere between approximately 300 and 600 hPa (Warner et

123 al., 2007; Warner et al., 2013; AIRS project., 2019). CO retrievals have a bias of 6-10% between

124 900 hPa and 300 hPa with a root mean square error of 8-12 % (McMillan et al., 2011).

125 Apart from MOPITT and AIRS CO data, we used Moderate Resolution Imaging

126 Spectroradiometer (MODIS) collection 6.1 daily active fire hot spot data from 2006–2020 over

127 Indonesia (Giglio et al., 2016).

2.3 MERRA-2 Reanalysis products

129 Modern-Era Retrospective Analysis for Research and Applications, version 2 (MERRA-2)

130 monthly mean geopotential height (GpH) wind vectors (zonal and meridional) and vertical

131 pressure velocity (omega) during the study period were utilized. MERRA-2 is the latest

132 atmospheric reanalysis data produced by the NASA Global Modeling and Assimilation Office

133 (GMAO) (Gelaro et al., 2017). The horizontal resolution of MERRA-2 reanalysis is 0.5º × 0.625º.

134 MERRA-2 data are available online through the NASA Goddard Earth Sciences Data Information

135 Services Center (GES DISC; https://disc.gsfc.nasa.gov/, last access: 11 September 2022).

136 **3. Results and Discussion**

137 **3.1 Higher CO mixing ratios in October 2006 and 2015 at LABS**

138   **Figure 2** summarizes the inter-annual variations of CO in October observed at LABS along

139 with MODIS active fire counts over Indonesia and the observed Niño 3.4 and the IOD index

140 values, which helped to motivate this study. The highest CO mixing ratios for this period were

141 observed in 2006 and 2015, well over the long-term means of 132.1±23.3ppb when including all

142 points and 126.8±19.6 ppb when excluding 2006 and 2015. A significant enhancement of CO, over

143 the latter mean calculation, of more than 47.2 ppb (37.2%) in 2006 and 36.7 ppb (28.9%) in 2015

144 was observed, with the value in 2006 (2015) more significant than the $\pm 2\sigma$ ($\pm 1\sigma$) standard

145 deviation of the long-term mean (**Table 1**). Higher CO mixing ratios in 2006 and 2015 at LABS

146 were also evident from the MOPITT and AIRS satellite measurements obtained over a 1-degree

147 radius around the LABS location (**Fig. 3**).

148   Unprecedented CO values in 2006 and 2015 at LABS could be due to the transport of CO

149 from large-scale forest fires that were intense during the same period in the Indonesian region. It

150 is clear from **Figure 2**, that the higher values of CO at LABS in 2006 and 2015 coincided with

151 more intense fire activity over Indonesia along with warm phases of ENSO and IOD (**Fig. 2c and**

152 **2d**), which have been extensively studied due to the induced drought conditions in those years

153 (Field et al., 2016; Huijnen et al., 2016; Pan et al., 2018). Several studies have reported on the

154 impact of the intense BB in 2006 and 2015 on the release of significant carbon emissions and the

155 air quality over the wider Equatorial Asian region (Logan et al., 2008; Chandra et al., 2009; Field

156 et al., 2016; Huijnen et al., 2016; Ravindra Babu et al., 2019). The enhanced CO values from the

157 2006 and 2015 events at LABS in the present study complement the findings of Matsueda and

158 Inoue (1999) in the case the of 1997 El Niño event and Nara et al. (2011) in the case of 2006 El

159 Niño event. However, the impact on CO at LABS occurred significantly further north of the source

160 region than in either of the aforementioned studies. Based on aircraft measurements, Matsueda and

161 Inoue (1999) reported the enhancement of CO_2, CO, and CH_4 in the upper troposphere (at 9-12

162 km) over the South China Sea (SCS) during October 1997 Indonesian fire event. However, this

163 large CO increase appeared only over the SCS west of Kalimantan and not in the subtropics

164 between10°N and 26°N. Nara et al. (2011) reported a substantial increase in CO mixing ratios over

165 the Western Tropical Pacific Ocean (between 15°N and the Equator) by shipboard observations

166 routinely operated between Japan and Australia and New Zealand during October and November

167 of 2006. Similarly, Pochanart and Akimoto (2003) also reported the influence of the 1997

168 Indonesian fire event on CO enhancement at the rural station Srinakarin (14°220N, 99°070E, 296

169 m above sea level) in Thailand.

170 In addition, due to La Niña and the negative phase IOD, the fire activity in Indonesia during

171 2016 was much less intense than in 2006 and 2015 (**Fig. 2c** and **2d**). Interestingly, CO at LABS

172 during 2016 exhibited the lowest October values in the entire data period, ~39.8 ppb (31.4%) lower

173 than the long-term October mean (2006-2021). It is well known that the major sources of CO at

174 LABS are BB from peninsular SEA in spring and industrial emissions from continental Asia in

175 winter (Ou-Yang et al., 2014; Pani et al., 2019; Ravindra Babu et al., 2022; Ou-Yang et al., 2022).

176 However, October is a transition month from the summer to winter at LABS, when air masses can

177 still arrive from the Pacific Ocean. Our analysis (**Fig. 2**) suggests that the extensive fires that

178 occurred during the 2006 and 2015 El Niño events over Indonesia may have yielded the

179 unprecedented CO mixing ratios at LABS in October of those years. Combined El Niño and IOD-

180 related changes in the large-scale dynamics and circulations may have promoted CO emissions

181 from Indonesian fires to transport to LABS.

Atmospheric
Chemistry
and Physics
Discussions

Open Access

EGU
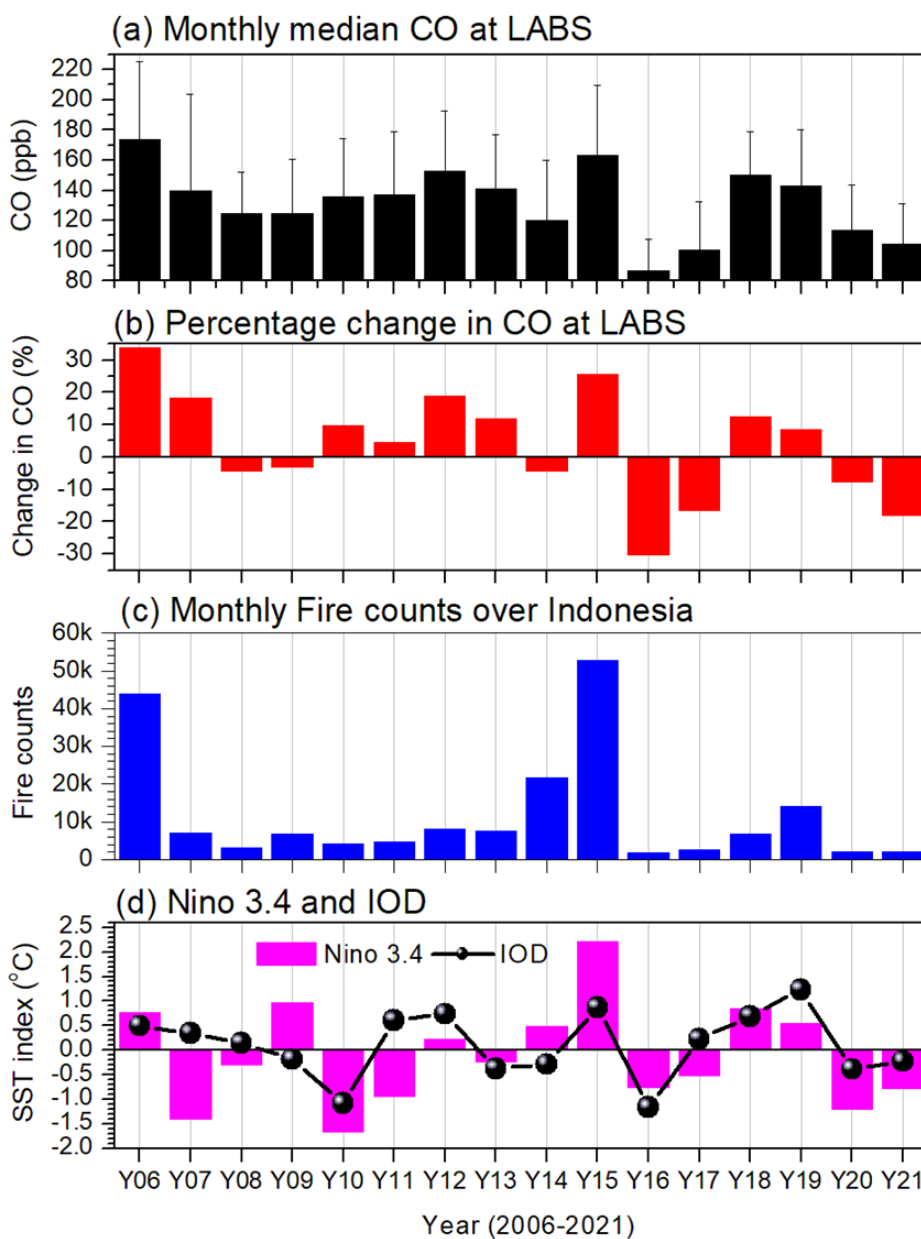
Figure 2. Inter-annual variations in October of the (a) monthly median of CO, (b) percentage change in CO from the long-term mean at LABS, (c) MODIS (Moderate Resolution Imaging Spectroradiometer) total active fire counts (only fires tagged with >30 % confidence) over

Indonesia, (d) sea surface temperature index for Niño 3.4 (magenta) and Indian ocean dipole (black) during 2006 to 2021.
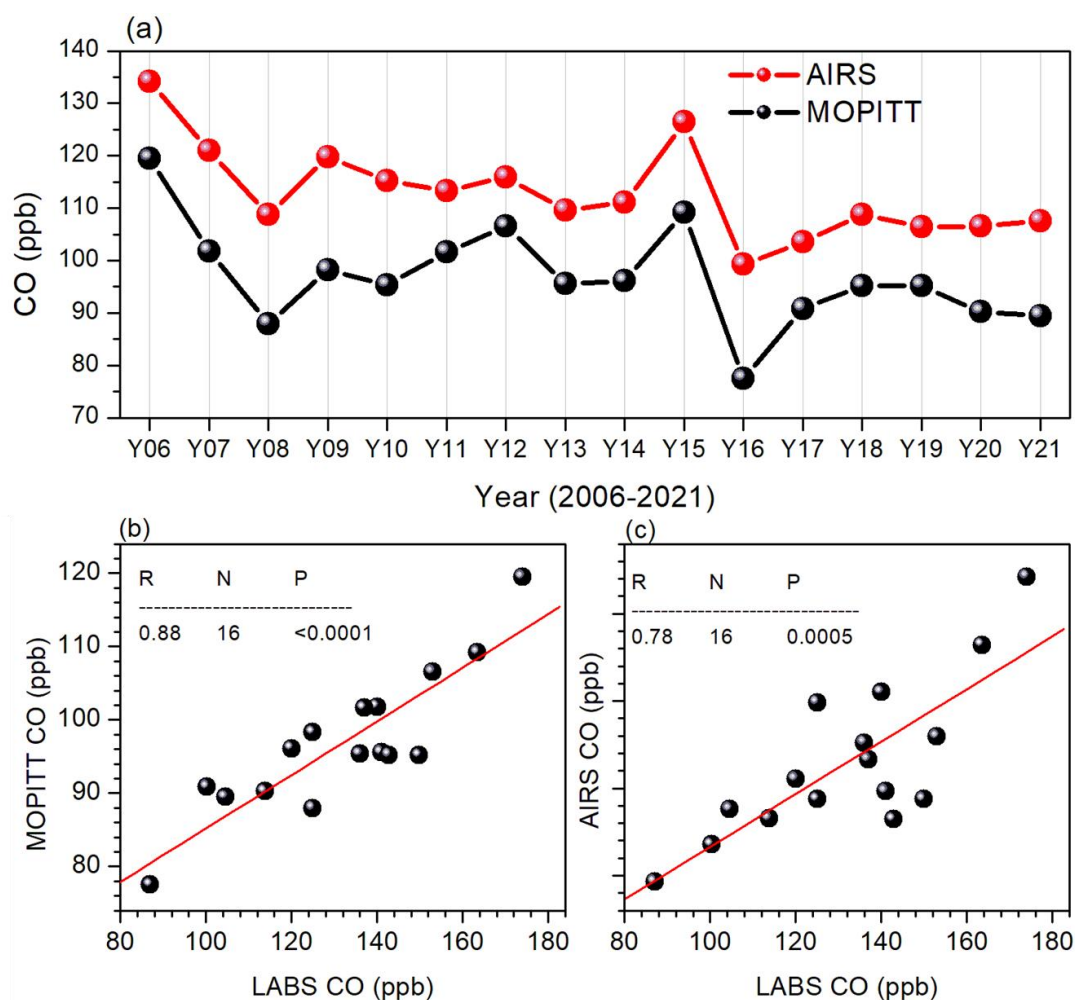
Figure 3. (a) MOPITT (black) and AIRS (red) satellite observed CO mixing ratios within the 1-degree radius around the LABS location, (b) correlation plot between in-situ CO at LABS and MOPITT CO, and (c) correlation plot between in-situ CO at LABS and AIRS CO in October month during 2006 to 2021. (R is the correlation coefficient; N is the sample size; P is the significance value)

196

197   To confirm the impact of Indonesian fire pollution on LABS CO, we further checked the

198   spatial distribution of CO in 2006 and 2015 from the MOPITT satellite CO observations. An inter-

199   comparison between October monthly mean CO at LABS (2006-2021) and MOPITT and AIRS

200   CO data within the 1-degree radius around the LABS location yielded correlation coefficients of

201   0.88 and 0.78 ($p<0.01$), respectively (**Fig. 3**). We then used the MOPITT satellite data to track the

202   spatial and vertical CO changes in October 2006 and 2015; first, we examined the distribution of

203   the CO anomalies at free tropospheric heights in those years. **Figure 4** shows these anomalies

204   compared to the long-term mean (2001-2021) at 700 hPa and 500 hPa, revealing extensive

205   enhancements of CO mixing ratios over most of equatorial Asia in 2006 and 2015. **Figure 4**

206   indicates that CO from the Indonesian fires affected both the Indian Ocean to the west and South

207   Pacific and the northern Pacific to the east. Furthermore, these outflows of CO split northwestward

208   into the Bay of Bengal and northeastward into the western North Pacific. It is also worth noting

209   that the anomalies were significantly higher at 500 hPa than 700 hPa. Elevated CO is visible in the

210   Taiwan region at 700 hPa and 500 hPa in both years. This further provides a clear signature of the

211   impact of Indonesian fire activity on enhanced CO in 2006 and 2015 at LABS. Overall, from

212   **Figure 4**, MOPITT CO data shows the Indonesia fires transported CO vertically and horizontally

213   in all directions. We further investigated the associated dynamics and large-scale circulations

214   supporting the transport of Indonesian pollution to LABS.
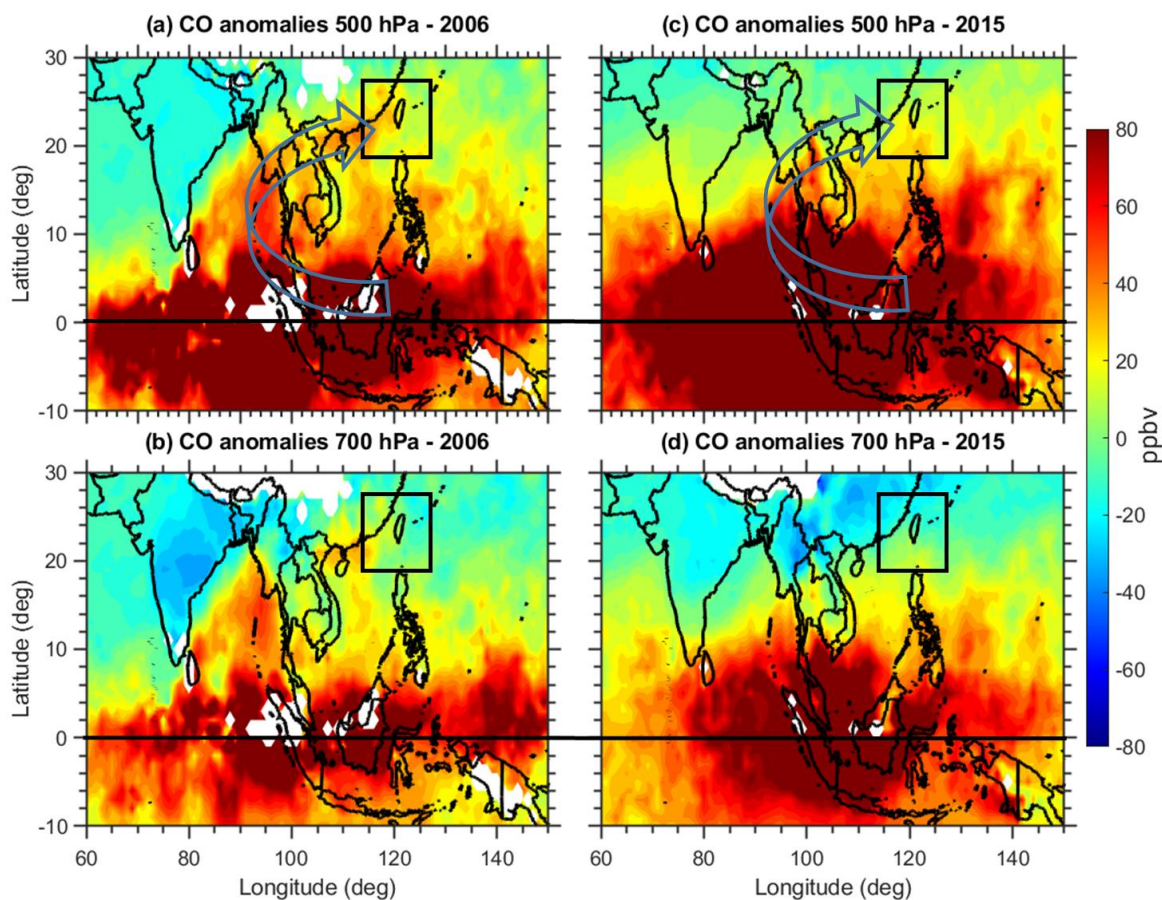
Figure 4. Monthly mean CO anomalies obtained from MOPITT satellite observations (a) at 500 hPa and (b) at 700 hPa during October 2006. Subplots (c) and (d) are the same as subplots (a) and (b) but for October 2015, respectively. The anomalies are obtained by subtracting the 2006 and 2015 data from the long-term mean of MOPITT CO data from 2001-to 2021.

3.2 Role of large-scale dynamics and atmospheric circulations

Large-scale dynamics and circulations can play a crucial role in transporting Indonesian pollution to long-distance downwind regions (Bowman, 2006; Nara et al., 2011; Matsueda et al., 2019). To understand the plausible mechanisms behind the transport of Indonesian fire pollution to LABS, we further examined the MERRA-2 reanalysis of geopotential height (GpH) and wind distribution in 2006 and 2015. The spatial distribution of GPH at two pressure levels (700 and 500 hPa) in both events is shown in **Figure 5**. The GpH and wind vectors in the two event years

227 exhibited quite different patterns in relation to a high-pressure system over the northern parts of
228 the SCS. A high-pressure anti-cyclonic circulation center extended from the Indo-China Peninsula
229 to the SCS in October 2006 with LABS located precisely on the eastern edge of the anticyclone.
230 In 2015, the anticyclone extended from the Indo-China Peninsula to the western North Pacific
231 region and over Taiwan.

232
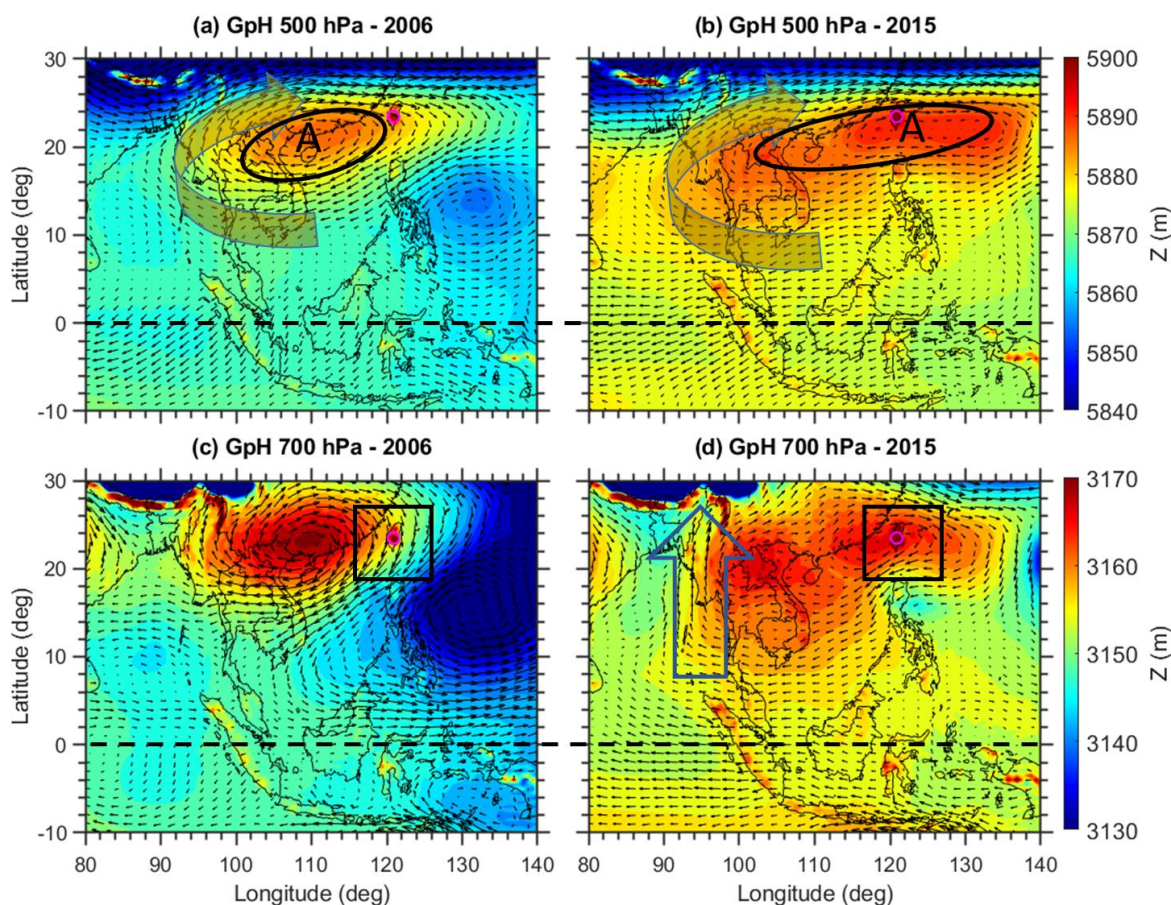
Figure 5. Monthly mean Geopotential height (GpH) obtained from MERRA-2 reanalysis (a) at
500 hPa and (b) at 700 hPa during October 2006. Subplots (c) and (d) are the same as subplots (a)
and (b) but for October 2015.

236 During both event years, strong southerlies at 500 hPa were evident due to the high-
237 pressure anticyclone system in the northern SCS. It is assumed that the northern edge of the
238 Indonesian fire pollution plume can be carried out by the southerlies and around the western edge

239   of the high-pressure anti-cyclone over SCS. An apparent merging of the southerlies from the

240   equator with the subtropical westerlies in the northern PSEA region subsequently led to the

241   transport of CO to downwind LABS. Overall, in both events, there was a significant anticyclone

242   over the SCS. El Niño and the positive IOD-induced high-pressure anticyclone over SCS

243   strengthen the southerlies from the equator, consequently bringing higher amounts of CO to LABS.

244   We further investigated the vertical pressure velocity (omega) behavior in both events (**Fig. 6**),

245   where negative (positive) values represent upward (downward) winds. Significant upward wind in

246   both events was evident over equatorial MC, while vertical pressure velocity over Taiwan and

247   surrounding regions at both pressure levels were mostly downwards in 2006 and 2015. The

248   presence of a downwind will provide downward transport of any pollutant presence in the upper

249   troposphere over that region. Also, the downward wind was relatively higher in 2006 compared to

250   2015. The center of the downward wind was shifted eastwards in the western North Pacific in

251   2015. The distinct behavior of vertical pressure velocity at the LABS region during the two events

252   might be due to the associated climate conditions in the two periods; more discussion will be

253   provided in section 3.4.

254
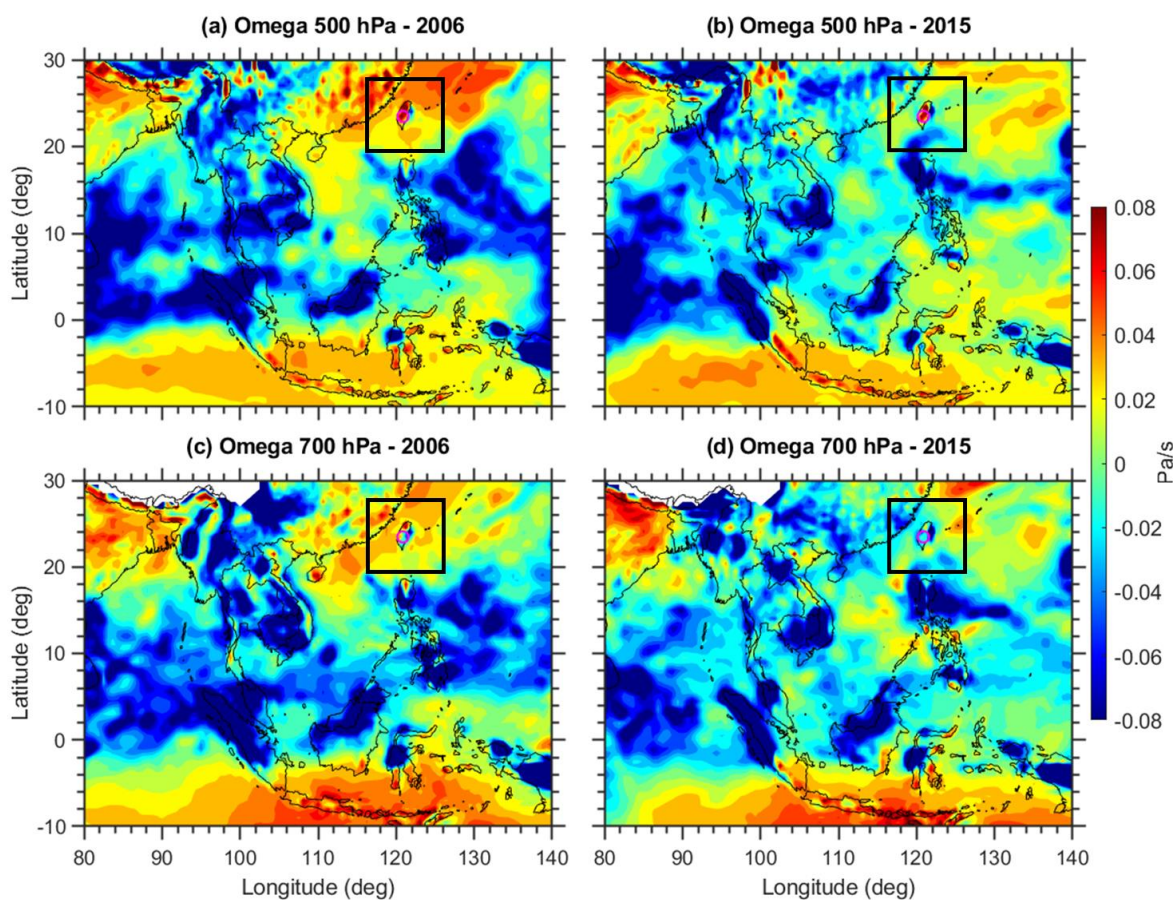
Figure 6. Monthly mean vertical pressure velocity obtained from MERRA-2 reanalysis (a) at 500
hPa and (b) at 700 hPa during October 2006. Subplots (c) and (d) are the same as subplots (a) and
(b) but for October 2015.

258   We further showed CO deviations at both pressure levels in October 2016 when there was

259   very low fire activity in Indonesia (**Fig. 7**). Interestingly, there was a significant lowering of CO

260   over the Taiwan region in 2016, which agrees with the observed low CO values from the in-situ

261   measurements at LABS (**Fig. 2b**). Also in agreement, 2016 was a La Niña and negative IOD year

262   and fire activity was much weaker (**Fig. 2c** and **2d**). During the La Niña years, large-scale

263   dynamical processes are greatly reversed with respect to El Niño years. We further analyzed the

264   GpH and wind circulation patterns in 2016 (**Fig. 8**). A significant high-pressure system (western

265   North Pacific subtropical High) was present over the western North Pacific region in 2016, which

266   was shifted considerably further eastward compared to over the SCS in 2006 and 2015. The wind

267   vectors also highlighted the transport of a clean marine air mass from the Pacific Ocean to LABS

268   in 2016. Interestingly, the vertical pressure velocity exhibited a pronounced upward wind over

269   Taiwan in 2016, in contrast to the downward wind in 2006 and 2015. This indicates that dominant

270   clean marine air reached LABS in 2016 resulting in the lowest CO mixing ratio in the entire dataset

271   at LABS.
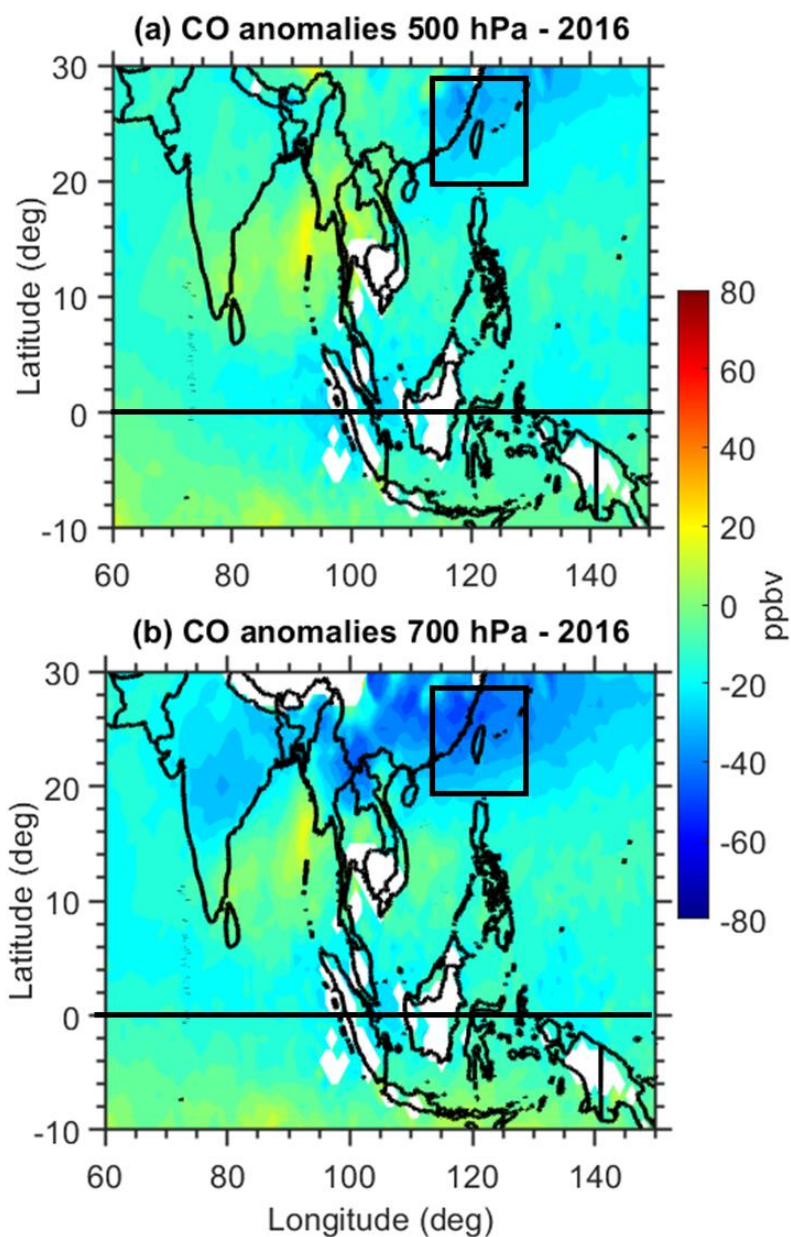
Figure 7. Monthly mean CO deviations from the long-term mean (2001-2021) were obtained from MOPITT satellite observations (a) at 500 hPa and (b) at 700 hPa during October 2016.
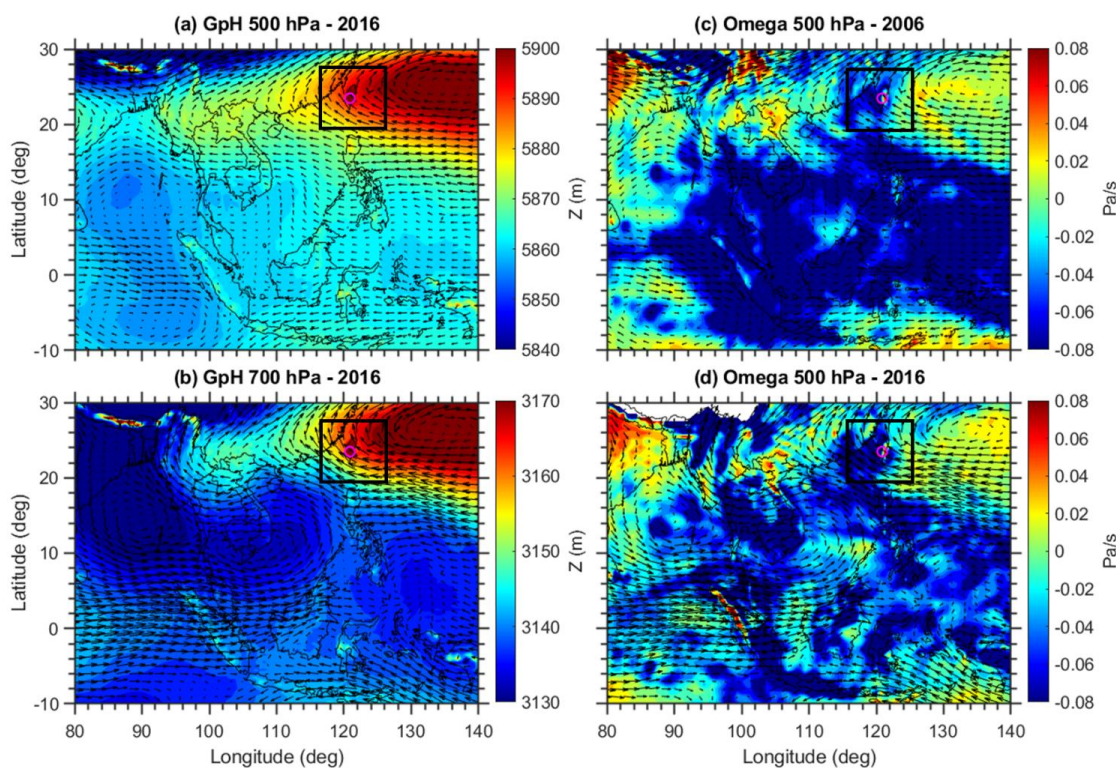
Figure 8. Monthly mean Geopotential height (GpH) obtained from MERRA-2 reanalysis (a) at
500 hPa, and (b) at 700 hPa during October 2016. The subplots (c) and (d) are the same as subplots
(a) and (b) but for the observed vertical pressure velocity (Omega).

3.4 Role of Hadley circulation

The Hadley circulation (HC) is a crucial component of the climate system, which is
characterized by a thermally driven large-scale meridional circulation (Hadley, 1735). This
circulation links the troposphere and stratosphere and the tropics and extra-tropics, through
horizontal and vertical motions, transporting moisture, heat, and momentum to regulate Earth's
energy budget. As the CO sources (Indonesia) in this study were close to the equator, it is expected
that air tends to rise more or less directly over the CO sources. **Figure 9** shows the vertical-
meridional cross-section of CO and vertical pressure velocity in separate panels averaged along
110°–130°E in October 2006 and 2015. The black-colored vertical line in all the panels in **Figure
9** shows the location of LABS and the horizontal line represents the 700 hPa. The vertical cross-
section of CO highlights the uplifting of CO into the upper troposphere over the equator, followed

290 by southward and northward movement in both 2006 and 2015 (**Fig. 9a** and **9b**). A clear transport

291 of CO from the source region to the sub-tropics via meridional transport was evident in both events.

292 It is noted that the higher CO observed between 20–30°N latitude below ~700 hPa is related to

293 anthropogenic emissions and not due to the Indonesian fires. To confirm the lofted CO from

294 Indonesia is really descended in the subtropics due to the Hadley circulation, we looked into the

295 vertical cross-section of vertical pressure velocity in both events. From Figure 8, it is suggested

296 that large amounts of CO from Indonesia were transferred into the free troposphere by the strong

297 upward air motion in this region. Similarly, there was a pronounced descending motion (positive

298 values of vertical pressure velocity) during October 2006 (**Fig. 9c**) in the northern hemisphere

299 subtropics around 20–30°N latitude, which corresponds well with the location of LABS. However,

300 in October 2015, the descending motion was not significant compared to 2006. This may be due

301 to the different El Niño conditions in 2006 and 2015. While IOD conditions were indeed similar

302 between 2006 and 2015 (**Fig. 2d**), the higher descending motions in 2006 can be explained in part

303 by the moderate El Niño conditions during that year. A well-developed El Niño condition was

304 already established in 2015 compared to 2006. In October 2006, the observed Niño 3.4 value was

305 around 0.7 whereas in 2015 it was around 2.21. These values indicate that the El Niño conditions

306 were already well established in October 2015 whereas, in 2006, the conditions were not developed

307 as El Niño. It is reported that in El Niño conditions, the western Pacific HC is observed to be

308 weakened whereas the eastern Pacific HC is strengthened (Wang, 2004). This is supported by the

309 observed lesser descending motions in 2015 from the present study. These differences in the

310 descending motions likely influenced the greater CO enhancement in 2006 compared to 2015 at

311 LABS (**Fig. 2b** and **Table 1**). Overall, it is clearly illustrated from the MOPITT CO vertical cross-

312 section and the MERRA-2 vertical pressure velocity that the CO emitted from the Indonesian fire

313 was transported vertically through the Hadley circulation to the LABS location.
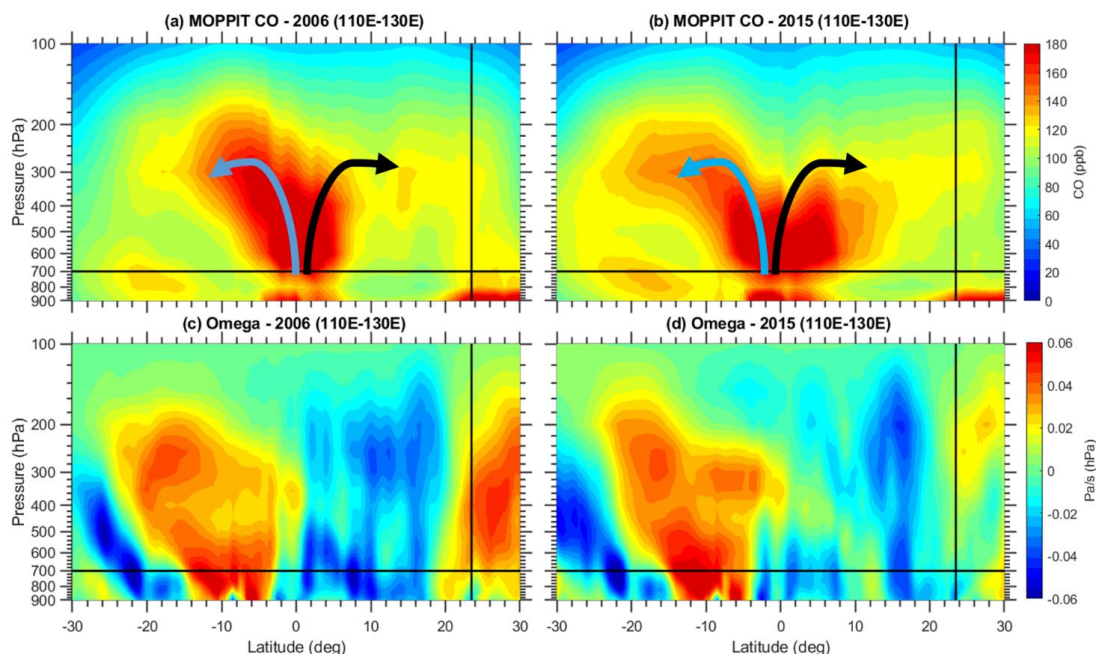
314

315 **Figure 9**. Vertical–meridional cross-section of MOPITT CO averaged along 110°–130°E (a) for

316 October 2006 and (b) for October 2015. Subplots (c) and (d) are the same as subplots (a) and (b)

317 but for the MERRA-2 reanalysis vertical pressure velocity. Positive (negative) values represent

318 the downward (upward) wind.

319 **4. Summary and Conclusions**

320   Changes in the background climate will inevitably impact meteorological transport

321 processes and the concentrations of pollutants arriving at downwind regions. Lulin Atmospheric

322 Background Station (LABS, 23.47°N 120.87°E, 2862 m ASL) is the only high-altitude background

323 station located in the western North Pacific region, and is optimally located to study some of these

324 transport processes, including long-range transport of pollution in the free troposphere and

325 stratospheric intrusions. During October 2006 and 2015, there were substantial increases in CO

326 mixing ratios, ~47.2 ppb (37.2%) and ~36.7 ppb (28.9%) increase compared to the 16-year (2006-

327 2021) means at LABS. Interestingly, these two events (2006 and 2015) were strongly associated

328 with the two major biomass burning episodes over Indonesia, which resulted from a combined

329 impact of positive phase ENSO and IOD-induced drought conditions. MODIS active fire counts

330 showed the largest fires in October 2006 and 2015 compared to the other years in the 16-year

331 period in Indonesia. These record fires reflected two of the largest carbon emissions in the

332 Indonesian region since 1997. Apart from these high values in October 2006 and 2015, in October

333 2016, extremely low CO values were recorded at LABS (~31.4% lower compared to 2006-2021

334 mean). October 2016 was associated with negative IOD over the Indian Ocean and La Niña in the

335 Pacific Ocean, resulting in the lowest fire activity over the MC. Further, we found that the large-

336 scale circulations in 2016 were quite different from 2006 and 2015. In 2016, LABS was dominated

337 by the southerlies due to the western Pacific subtropical High (WPSH), which transported clean

338 marine air from the Pacific Ocean and caused record low CO values at LABS. The main aim of

339 our study was to examine the transport pathways of CO from Indonesia's source region to the

340 downwind LABS region. By comparing the CO and atmospheric circulation data from the 2006

341 and 2015 El Niño (positive IOD) years and 2016 La Niña (negative IOD), we found two plausible

342 transport pathways of CO from Indonesia to LABS.

343 **Figure 10** illustrates a schematic diagram of the major transport pathways of CO from

344 Indonesia to subtropical East Asia during the two event years. They include horizontal transport

345 in the free troposphere due to El Niño-induced high-pressure anticyclone circulation and vertically

346 through the Hadley circulation. For October 2006 and 2015, corresponding to El Niño and positive

347 IOD, northern SCS was influenced by the high-pressure anti-cyclonic system in the free

348 troposphere. The southerlies on the southwest flank of the anticyclone further merged with the

349 subtropical westerlies over PSEA and then transported polluted air to LABS. Apart from this

350 horizontal transport, CO was transported through the Hadley circulation to LABS in both events.

351 However, there was a distinctly different HC strength in 2006 compared to 2015 due to the

352 different El Niño conditions. These two events were strongly associated with positive IOD, but in

353 2006, the El Niño conditions were not well developed, whereas in 2015 well-developed El Niño

354 conditions were evident. These El Niño conditions further suppressed the HC over the western

355 Pacific in 2015 compared to 2006. This suggested the importance of the background climate

356 conditions (ENSO and IOD) on the pollutant transport process. A changing warmer climate can

357 influence carbon emissions and alter the transport pathways, hence impacting the various scales of

358 air pollution and climate. Overall, the present results further provide knowledge to the atmospheric

359 chemistry community about the different transport pathways of pollutants and the role of climate

360 conditions.

Atmospheric
Chemistry
and Physics

Discussions

Open Access

EGU
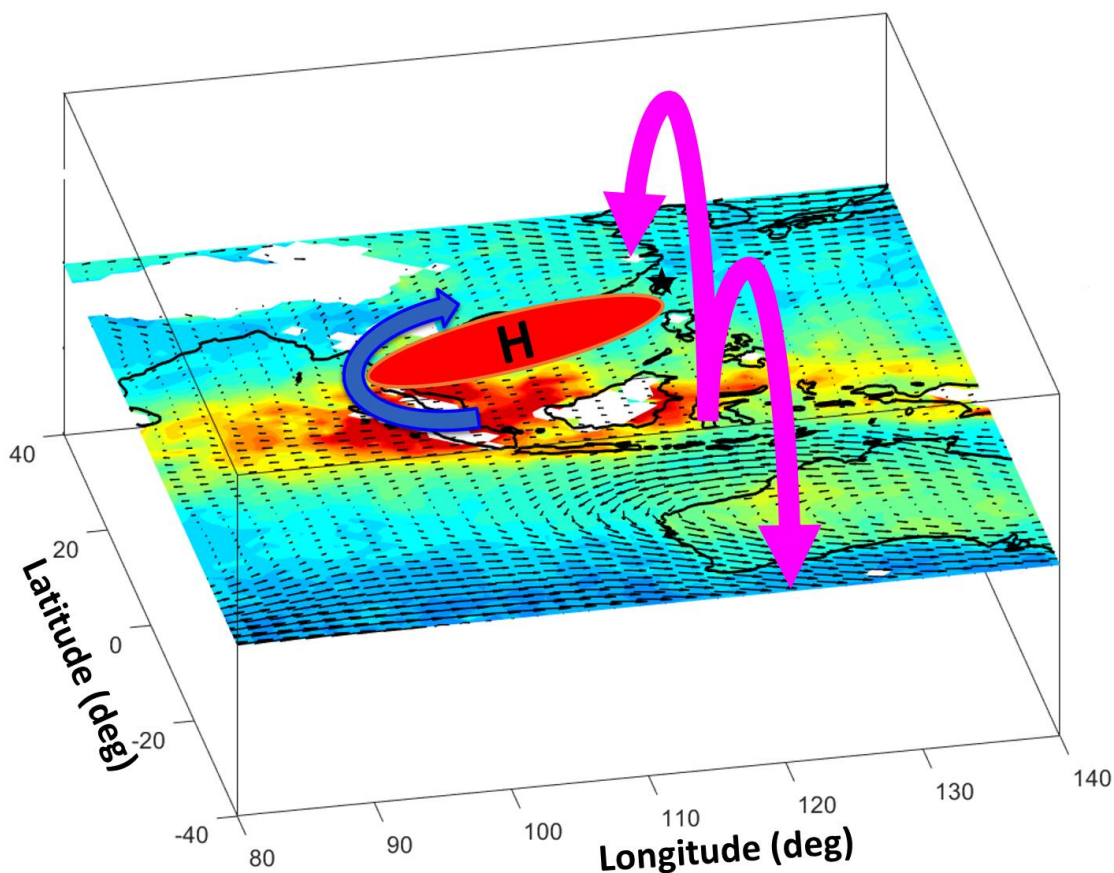
Figure 10. Schematic diagram of CO transport from Indonesian fires to subtropical East Asian region. Horizontal transport of CO due to the high-pressure anticyclone is denoted by the blue-colored arrow. H denotes high-pressure anticyclone over northern parts of the South China Sea. Magenta-colored arrows indicate the transport of CO through the local Hadley circulation (over 110°–130°E). Black-colored star symbol represents the LABS location.

Data availability

The CO data at LABS can be assessed at http://lulin.tw/index_en.htm. The AIRS and MOPITT CO data can be downloaded from the following websites https://disc.gsfc.nasa.gov/datasets/AIRS3STM_7.0 (AIRS project., 2019) and https://asdc.larc.nasa.gov/project/MOPITT. MERRA-2 data are available online through the

Atmospheric
Chemistry
and Physics
Discussions

372   NASA Goddard Earth Sciences Data Information Services Center (GES DISC;
373   https://disc.gsfc.nasa.gov, last access: 30 May 2022). Nino 3.4 Index and IOD data can be
374   downloaded through the following websites https://psl.noaa.gov/gcos_wgsp/Timeseries/Niño34/.
375   https://psl.noaa.gov/gcos_wgsp/Timeseries/DMI/. The MODIS fire products can be downloaded
376   from the following website https://firms.modaps.eosdis.nasa.gov/active_fire/.

377   **Author contributions**

378   **Saginela Ravindra Babu:** Conceptualization, Data curation, Formal analysis, Investigation,
379   Software, Validation, Visualization, Writing – original draft preparation, Writing – review and
380   editing; **Chang-Feng Ou-Yang**: Data curation, Software, Validation, Visualization; **Stephen M.**
381   **Griffith**; Writing – review and editing; **Shantanu Kumar Pani**: Data curation and Visualization;
382   **Steven S. Kong**: Data curation and Visualization; **Neng-Huei Lin**: Conceptualization,
383   Investigation, Funding Acquisition, Supervision, Resources, Writing – review and editing.

384   **Competing Interest**

385   The authors declare that they have no conflict of interest.

386   **Acknowledgments**

397

398

399

Atmospheric
Chemistry
and Physics
Discussions

5. References

AIRS project (2019), Aqua/AIRS L3 Monthly Standard Physical Retrieval (AIRS-only) 1-degree x 1 degree V7.0, Greenbelt, MD, USA, Goddard Earth Sciences Data and Information Services Center (GES DISC), Accessed: (11 September 2022), 10.5067/UBENJB9D3T2H.

Bowman, K. P. and Cohen, P. J.: Interhemispheric exchange by seasonal modulation of the Hadley circulation, J. Atmos. Sci., 54, 2045–2059, https://doi.org/10.1175/1520-0469(1997)054%3C2045:IEBSMO%3E2.0.CO;2, 1997.

Bowman, K. P.: Transport of carbon monoxide from the tropics to the extratropics, J. Geophys. Res.-Atmos., 111, https://doi.org/10.1029/2005JD006137, 2006.

Chandra, S., Ziemke, J. R., Duncan, B. N., Diehl, T. L., Livesey, N. J. and Froidevaux, L.: Effects of the 2006 El Niño on tropospheric ozone and carbon monoxide: implications for dynamics and biomass burning, Atmos. Chem. Phys., 9, 4239–4249, https://doi.org/10.5194/acp-9-4239-2009, 2009.

Chandra, S., Ziemke, J. R., Schoeberl, M. R., Froidevaux, L., Read, W. G., Levelt, P.F. and Bhartia, P. K.: Effects of the 2004 El Nino on tropospheric ozone and water vapor, Geophys.Res. Lett., 34, L06802, https://doi.org/10.1029/2006GL028779, 2007.

Chi, K.H., Hung, N.T., Lin, C.Y., Wang, S.H., Ou-Yang, C.F., Lee, C.T. and Lin, N.H.: Evaluation of Atmospheric PCDD/Fs at Two High-Altitude Stations in Vietnam and Taiwan during Southeast Asia Biomass Burning. Aerosol Air Qual. Res. 16: 2706-2715. https://doi.org/10.4209/aaqr.2015.11.0653, 2016.

Chuang, M. T., Fu, J. S., Lee, C. Te, Lin, N. H., Gao, Y., Wang, S. H., Sheu, G. R., Hsiao, T. C., Wang, J. L., Yen, M. C., Lin, T. H. and Thongboonchoo, N.: The simulation of long-range transport of biomass burning plume and short-range transport of anthropogenic pollutants to a mountain observatory in east Asia during the 7-SEAS/2010 Dongsha experiment, Aerosol Air Qual. Res., 16(11), 2933–2949, https://doi.org/10.4209/aaqr.2015.07.0440, 2016.

Cheng, F.-Y., Yang, Z.-M., Ou-Yang, C.-F. and Ngan, F.: A numerical study of the dependence of long-range transport of CO to a mountain station in Taiwan on synoptic weather patterns

427   during the Southeast Asia biomass-burning season, Atmos. Environ., 78, 277–290,
428   https://doi.org/10.1016/j.atmosenv.2013.03.020, 2013.

429 Cooper, O. R., Gao, R. S., Tarasick, D., Leblanc, T., and Sweeney, C.: Long-term ozone trends at
430   rural ozone monitoring sites across the United States, 1990–2010, J. Geophys. Res.-
431   Atmos.,117, 1990–2010, https://doi.org/10.1029/2012JD018261, 2012.

432 Deeter, M. N., Edwards, D. P., Francis, G. L., Gille, J. C., Mao, D., Martínez-Alonso, S., Worden,
433   H. M., Ziskin, D., and Andreae, M. O.: Radiance-based retrieval bias mitigation for the
434   MOPITT instrument: the version 8 product, Atmos. Meas. Tech., 12, 4561–4580,
435   https://doi.org/10.5194/amt-12-4561-2019, 2019.

436 Doherty, R. M., Stevenson, D. S., Johnson, C. E., Collins, W. J., and Sanderson, M. G.:
437   Tropospheric ozone and El Nino-Southern Oscillation: Influence of atmospheric dynamics,
438   biomass burning emissions, and future climate change, J. Geophys. Res., 111, D19304,
439   https://doi.org/10.1029/2005JD006849, 2006.

440 Duncan, B. N., Bey, I., Chin, M., Mickley, L. J., Fairlie, T. D., Martin, R. V., and Matsueda, H.:
441   Indonesian wildfires of 1997: Impact on tropospheric chemistry, J. Geophys. Res., 108, 4458,
442   https://doi.org/10.1029/2002JD003195, 2003a.

443 Duncan, B. N., Martin, R. V., Staudt, A., et al.: Inter-annual and seasonal variability of biomass
444   burning emissions constrained by satellite observations, J. Geophys. Res., 108, 4100,
445   https://doi.org/10.1029/2002JD002378, 2003b.

446 Field, R. D., van der Werf, G. R., and Shen, S. S. P.: Human amplification of drought-induced
447   biomass burning in Indonesia since 1960, Nature Geoscience, 2, 185–188,
448   https://doi.org/10.1038/ngeo443,2009.

449 Field, R. D., van der Werf, G. R., Fanin, T., Fetzer, E. J., Fuller, R., Jethva, H., Levy, R., Livesey,
450   N. J., Luo, M., Torres, O., and Worden, H. M.: Indonesian fire activity and smoke pollution in
451   2015 show persistent nonlinear sensitivity to El Ni˜no-induced drought, Proceedings of the
452   National Academy of Sciences, 113, 9204–9209, https://doi.org/10.1073/pnas.1524888113,
453   2016.

454   Gelaro, R., McCarty, W., Suárez, M. J., Todling, R., Molod, A., Takacs, L., Randles, C. A.,
455   Darmenov, A., Bosilovich, M. G., Reichle, R., Wargan, K., Coy, L., Cullather, R., Draper, C.,
456   Akella, S., Buchard, V., Conaty, A., Silva, A. M. da, Gu, W., Kim, G.-K., Koster, R., Lucchesi,
457   R., Merkova, D., Nielsen, J. E., Partyka, G., Pawson, S., Putman, W., Rienecker, M., Schubert,
458   S. D., Sienkiewicz, M., and Zhao, B.: The Modern-Era Retrospective Analysis for Research
459   and Applications, Version 2 (MERRA-2), J. Climate, 30, 5419–5454,
460   https://doi.org/10.1175/jcli-d-16-0758.1, 2017.

461   Giglio, L., Schroeder, W., and Justice, C. O.: The collection 6 MODIS active fire detection
462   algorithm and fire products, Remote Sens. Environ., 178, 31–41,
463   https://doi.org/10.1016/j.rse.2016.02.054, 2016.

464   Hadley, G.: Concerning the cause of the general trade-winds. Philos. Trans. R. Soc. Lond. 29, 58–
465   62. https://doi.org/10.1098/rstl.1735.0014, 1735.

466   Heymann, J., Reuter, M., Buchwitz, M., Schneising, O., Bovensmann, H., Burrows, J. P., Massart,
467   S., Kaiser, J. W., and Crisp, D.: CO2 emission of Indonesian fires in 2015 estimated from
468   satellite-derived atmospheric CO2 concentrations, Geophys. Res. Lett., 44, 1537–1544,
469   https://doi.org/10.1002/2016gl072042, 2017.

470   Hsiao, T. C., Ye, W. C., Wang, S. H., Tsay, S. C., Chen, W. N., Lin, N. H., Lee, C. Te, Hung, H.
471   M., Chuang, M. T., and Chantara, S.: Investigation of the CCN activity, BC and UVBC mass
472   concentrations of biomass burning aerosols during the 2013 BASELInE campaign, Aerosol Air
473   Qual. Res., 16, 2742–2756, https://doi.org/10.4209/aaqr.2015.07.0447, 2016.

474   Huang, L., Lin, W., Li, F., Wang, Y. and Jiang, B.: Climate Impacts of the Biomass Burning in
475   Indochina on Atmospheric Conditions over Southern China. Aerosol Air Qual. Res. 19: 2707-
476   2720. https://doi.org/10.4209/aaqr.2019.01.0028, 2019.

477   Huang, H. Y., Wang, S. H., Huang, W. X., Lin, N. H., Chuang, M. T., da Silva, A. M. and Peng,
478   C. M.: Influence of Synoptic-Dynamic Meteorology on the Long-Range Transport of Indochina
479   Biomass Burning Aerosols, J. Geophys. Res. Atmos., 125(3),
480   https://doi.org/10.1029/2019JD031260, 2020.

481 Huijnen, V., Wooster, M. J., Kaiser, J. W., Gaveau, D. L. A., Flemming, J., Parrington, M., Inness,
482   A., Murdiyarso, D., Main, B., and van Weele, M.: Fire carbon emissions over maritime
483   southeast Asia in 2015 largest since 1997, Sci. Rep., 6, 26886,
484   https://doi.org/10.1038/srep26886, 2016.

485 Lin, C.-Y., Hsu, H.-m., Lee, Y. H., Kuo, C. H., Sheng, Y.-F., and Chu, D. A.: A new transport
486   mechanism of biomass burning from Indochina as identified by modeling studies, Atmos.
487   Chem. Phys., 9, 7901–7911, https://doi.org/10.5194/acp-9-7901-2009, 2009.

488 Lin, N.-H., Tsay, S.-C., Maring, H. B., Yen, M.-C., Sheu, G.-R., Wang, S.-H., Chi, K. H., Chuang,
489   M.-T., Ou-Yang, C.-F., Fu, J. S., Reid, J. S., Lee, C.-T., Wang, L.-C., Wang, J.-L., Hsu, C. N.,
490   Sayer, A. M., Holben, B. N., Chu, Y.-C., Nguyen, X. A., Sopajaree, K., Chen, S.-J., Cheng, M.-
491   T., Tsuang, B.-J., Tsai, C.-J., Peng, C.-M., Schnell, R. C., Conway, T., Chang, C.-T., Lin, K.-
492   S., Tsai, Y. I., Lee, W.-J., Chang, S.-C., Liu, J.-J., Chiang, W.-L., Huang, S.-J., Lin, T.-H. and
493   Liu, G.-R.: An overview of regional experiments on biomass burning aerosols and related
494   pollutants in Southeast Asia: From BASE-ASIA and the Dongsha Experiment to 7-SEAS,
495   Atmos. Environ., 78, 1–19, https://doi.org/10.1016/j.atmosenv.2013.04.066, 2013.

496 Lin, C. C., Chen, W. N., Loftus, A. M., Lin, C. Y., Fu, Y. T., Peng, C. M. and Yen, M. C.:
497   Influences of the long-range transport of biomass-burning pollutants on surface air quality
498   during 7-SEAS field campaigns, Aerosol Air Qual. Res., 17(10), 2595–2607,
499   https://doi.org/10.4209/aaqr.2017.08.0273, 2017.

500 Logan, J. A., Megretskaia, I., Nassar, R., Murray, L. T., Zhang, L., Bowman, K. W., Worden, H.
501   M., and Luo, M.: Effects of the 2006 El Niño on tropospheric composition as revealed by data
502   from the Tropospheric Emission Spectrometer (TES), Geophys. Res. Lett., 35, 1–5,
503   https://doi.org/10.1029/2007GL031698, 2008.

504 Matsueda, H. and Inoue, H. Y.: Aircraft measurements of trace gases between Japan and Singapore
505   in October of 1993, 1996, and 1997, Geophys. Res. Lett., 26, 2413–2416,
506   https://doi.org/10.1029/1999GL900089, 1999.

507 Matsueda, H., Inoue, H. Y., and Ishii, M.: Aircraft observation of carbon dioxide at 8–13 km
508   altitude over the western Pacific from 1993 to 1999, Tellus B, 54, 1–21,
509   https://doi.org/10.1034/j.1600-0889.2002.00304.x, 2002.

Matsueda, H., Buchholz, R. R., Ishijima, K., Worden, H. M., Hammerling, D., and Machida, T.:
Interannual Variation of Upper Tropospheric CO over the Western Pacific Linked with
Indonesian Fires, SOLA, 15, 205–210, https://doi.org/10.2151/sola.2019-037, 2019.

Nara, H., Tanimoto, H., Nojiri, Y., Mukai, H., Zeng, J., Tohjima, Y., and Machida, T.: CO
emissions from biomass burning in South-east Asia in the 2006 El Nino year: shipboard and
AIRS satellite observations, Environ. Chem., 8, 213–223, https://doi.org/10.1071/EN10113,
2011.

Nassar, R., Logan, J. A., Megretskaia, I. A., Murray, L. T., Zhang, L., and Jones, D. B. A.: Analysis
of tropical tropospheric ozone, carbon monoxide, and water vapor during the 2006 El Niño
using TES observations and the GEOS Chem model, J. Geophys. Res.-Atmos., 114, D17304,
https://doi.org/10.1029/2009JD011760, 2009.

Niwa, Y., Sawa, Y., Nara, H., Machida, T., Matsueda, H., Umezawa, T., Ito, A., Nakaoka, S.-I.,
Tanimoto, H., and Tohjima, Y.: Estimation of fire-induced carbon emissions from Equatorial
Asia in 2015 using in situ aircraft and ship observations, Atmos. Chem. Phys., 21, 9455–9473,
https://doi.org/10.5194/acp-21-9455-2021, 2021.

Ou-Yang, C. F., Lin, N. H., Lin, C. C., Wang, S. H., Sheu, G. R., Lee, C. Te, Schnell, R. C., Lang,
P. M., Kawasato, T. and Wang, J. L.: Characteristics of atmospheric carbon monoxide at a high-
mountain background station in East Asia, Atmos. Environ., 89, 613–622,
https://doi.org/10.1016/j.atmosenv.2014.02.060, 2014.

Ou-Yang, C. F., Ravindra Babu, S., Jia-Ren Lee, Ming-Cheng Yen, Stephen M. Griffith, Chia-
Ching Lin, Shuenn-Chin Chang and Neng-Huei Lin.: Detection of stratospheric intrusion events
and their role in ozone enhancement at a mountain background site in sub-tropical East Asia,
Atmos. Environ., 268, 118779, https://doi.org/10.1016/j.atmosenv.2021.118779, 2022.

Pani, S. K., Wang, S. H., Lin, N. H., Lee, C. Te, Tsay, S. C., Holben, B. N., Janjai, S., Hsiao, T.
C., Chuang, M. T. and Chantara, S.: Radiative effect of springtime biomass-burning aerosols
over northern Indochina during 7-SEAS/BASELInE 2013 campaign, Aerosol Air Qual. Res.,
16(11), 2802–2817, https://doi.org/10.4209/aaqr.2016.03.0130, 2016.

Atmospheric
Chemistry
and Physics
Discussions

537 Pani, S. K., Ou-Yang, C.-F., Wang, S.-H., Ogren, J. A., Sheridan, P. J., Sheu, G.-R., and Lin, N.-
538　　H. J. A. E.: Relationship between long-range transported atmospheric black carbon and carbon
539　　monoxide at a high-altitude background station in East Asia, Atmos. Environ, 210, 86-99,
540　　https://doi.org/10.1016/j.atmosenv.2019.04.053, 2019.

541 Pan, X., Chin, M., Ichoku, C. M., and Field, R. D.: Connecting Indonesian fires and drought with
542　　the type of El Niño and phase of the Indian Ocean dipole during 1979–2016, J. Geophys. Res.-
543　　Atmos., 123, 1–15, https://doi.org/10.1029/2018JD028402, 2018.

544 Park, S., Kim, S.W., Lin, N.H., Pani, S.K., Sheridan, P.J. and Andrews, E.: Variability of Aerosol
545　　Optical Properties Observed at a Polluted Marine (Gosan, Korea) and a High-altitude Mountain
546　　(Lulin, Taiwan) Site in the Asian Continental Outflow. Aerosol Air Qual. Res. 19: 1272-1283.
547　　https://doi.org/10.4209/aaqr.2018.11.0416, 2019.

548 Parker, R. J., Boesch, H., Wooster, M. J., Moore, D. P., Webb, A. J., Gaveau, D., and Murdiyarso,
549　　D.: Atmospheric CH4 and CO2 enhancements and biomass burning emission ratios derived
550　　from satellite observations of the 2015 Indonesian fire plumes, Atmos. Chem. Phys., 16, 10111–
551　　10131, https://doi.org/10.5194/acp-16-10111-2016, 2016.

552 Pochanart, P., Akimoto, H., Kajii, Y., and Sukasem, P.: Carbon monoxide, regional-scale, and
553　　biomass burning in tropical continental Southeast Asia: Observations in rural Thailand, J.
554　　Geophys. Res.-Atmos., 108, 4552, https://doi.org/10.1029/2002JD003360, 2003.

555 Ravindra Babu, S., VenkataRatnam, M., Basha, G., Liou, Y.-A., and Narendra Reddy, N.: Large
556　　Anomalies in the Tropical Upper Troposphere Lower Stratosphere (UTLS) Trace Gases
557　　Observed during the Extreme 2015–16 El Niño Event by Using Satellite Measurements,
558　　Remote Sensing, 11, 687, https://doi.org/10.3390/rs11060687, 2019.

559 Ravindra Babu, S., Nguyen, L. S. P., Sheu, G.-R., Griffith, S. M., Pani, S. K., Huang, H.-Y., and
560　　Lin, N.-H.: Long-range transport of La Soufrière volcanic plume to the western North Pacific:
561　　Influence on atmospheric mercury and aerosol properties, Atmos. Environ., 268, 118806,
562　　https://doi.org/10.1016/j.atmosenv.2021.118806, 2022.

563 Reid, J. S., Hyer, E. J., Johnson, R., Holben, B. N., Yokelson, R. J., Zhang, J., Campbell, J. R.,
564　　Christopher, S. A., Di Girolamo , L., Giglio, L., Holz, R. E., Kearney, C., Miettinen, J., Reid,

E. A.,Turk, F. J., Wang, J., Xian, P., Zhao, G., Balasubramanian, R., Chew, B. N., Janai, S., Lagrosas, N., Lestari, P., Lin, N.-H., Mahmud, M., Nguyen, A. X., Norris, B., Oahn, N. T. K., Oo, M., Salinas, S. V., Welton, E. J., Liew, S. C.: Observing and understanding the Southeast Asian aerosol system by remote sensing: An initial review and analysis for the Seven Southeast Asian Studies (7SEAS) program, Atmos. Res., 122, 403-468, https://doi.org/10.1016/j.atmosres.2012.06.005, 2013.

Tsay, S. C., Maring, H. B., Lin, N. H., Buntoung, S., Chantara, S., Chuang, H. C., Gabriel, P. M., Goodloe, C. S., Holben, B. N., Hsiao, T. C., Christina Hsu, N., Janjai, S., Lau, W. K. M., Lee, C. Te, Lee, J., Loftus, A. M., Nguyen, A. X., Nguyen, C. M., Pani, S. K., Pantina, P., Sayer, A. M., Tao, W. K., Wang, S. H., Welton, E. J., Wiriya, W. and Yen, M. C.: Satellitesurface perspectives of air quality and aerosol-cloud effects on the environment: An overview of 7-SEAS/BASELInE, Aerosol Air Qual. Res., 16(11), 2581–2602, https://doi.org/10.4209/aaqr.2016.08.0350 , 2016.

van der Werf, G. R., Dempewolf, J., Trigg, S. N., Randerson, J. T., Kasibhatla, P. S., Giglio, L., Murdiyarso, D., Peters, W., Morton, D. C., Collatz, G. J., Dolman, A. J., and DeFries, R. S.: Climate regulation of fire emissions and deforestation in equatorial Asia, Proc. Natl. Acad. Sci. USA, 105, 20350–20355, https://doi.org/10.1073/pnas.0803375105, 2008.

van der Werf, G. R., Randerson, J. T., Giglio, L., van Leeuwen, T. T., Chen, Y., Rogers, B. M., Mu, M., van Marle, M. J. E., Morton, D. C., Collatz, G. J., Yokelson, R. J., and Kasibhatla, P. S.: Global fire emissions estimates during 1997–2016, Earth Syst. Sci. Data, 9, 697–720, https://doi.org/10.5194/essd-9-697-2017, 2017.

Wang, C.: ENSO, Atlantic climate variability, and the Walker and Hadley circulations, in: The Hadley circulation: Present, past and future, Springer, Berlin, 173–202, https://doi.org/10.1007/978-1-4020-2944-8_7, 2004.

Wang, S.-H., Welton, E. J., Holben, B. N., Tsay, S.-C., Lin, N.-H., Giles, D., Stewart, S. A., Janjai, S., Nguyen, X. A., Hsiao, T.-C., Chen, W.-N., Lin, T.-H., Buntoung, S., Chantara, S., and Wiriya, W.: Vertical Distribution and Columnar Optical Properties of Springtime Biomass-Burning Aerosols over Northern Indochina during 2014 7-SEAS Campaign, Aerosol Air Qual. Res., 15, 2037–2050, https://doi.org/10.4209/aaqr.2015.05.0310, 2015.

594   Weng, H. Y., Behera, S. K., and Yamagata, T.: Anomalous winter climate conditions in the Pacific
595   rim during recent El Niño Modoki and El Niño events, Clim. Dynam., 32, 663–674,
596   https://doi.org/10.1007/s00382-008-0394-6, 2009.

597   Whitburn, S., Van Damme, M., Clarisse, L., Turquety, S., Clerbaux, C., and Coheur, P.-F.:
598   Doubling of annual ammonia emissions from the peat fires in Indonesia during the 2015 El
599   Niño, Geophys. Res. Lett., 43, 11007–11014, https://doi.org/10.1002/2016gl070620, 2016.

600   Worden, J., Jiang, Z., Jones, D. B. A., Alvarado, M., Bowman, K., Frankenberg, C., Kort, E. A.,
601   Kulawik, S. S., Lee, M., Liu, J., Payne, V., Wecht, K., and Worden, H.: El Niño, the 2006
602   Indonesian peat fires, and the distribution of atmospheric methane, Geophys. Res. Lett., 40,
603   4938–4943, https://doi.org/10.1002/grl.50937, 2013.

604   Yin, Y., Ciais, P., Chevallier, F., van der Werf, G. R., Fanin, T., Broquet, G., Boesch, H., Cozic,
605   A., Hauglustaine, D., Szopa, S., and Wang, Y.: Variability of fire carbon emissions in equatorial
606   Asia and its nonlinear sensitivity to El Niño, Geophys. Res. Lett., 43, 10472–10479,
607   https://doi.org/10.1002/2016gl070971, 2016.

608

609

610   **Table 1**. Detailed statistics of observed CO in October during 2006 to 2021 at LABS.

Year	Mean	Median	Standard Deviation	Change in CO (%)	Total data points
2006	**175.8**	**174**	**51**	**33.9**	**703**
2007	155.3	140	63.4	18.3	732
2008	125.5	125	26.9	-4.4	599
2009	127.1	125	35.5	-3.2	533
2010	143.9	136	38.1	9.6	739
2011	137.1	137	41.9	4.4	734
2012	155.8	153	39.4	18.7	643
2013	146.8	141	35.7	11.8	365
2014	125.6	120	39.8	-4.2	602
2015	**164.8**	**163.5**	**46.2**	**25.6**	**732**
2016	91.6	87	20.9	-30.2	732
2017	109.7	100.3	32.4	-16.4	744
2018	147.7	149.9	29.1	12.5	736
2019	142.4	142.8	37.7	8.5	742
2020	121.3	113.8	29.5	-7.5	742
2021	107.7	104.6	26.9	-17.9	744

611